Supplementary for

Method to Quantify the Black Carbon Aerosol Light Absorption Enhancement with Entropy and Diversity Measures

Gang Zhao[1], Tianyi Tan[1], Yishu Zhu[1], Min Hu[1], Chunsheng Zhao[2*]

1 State Key Joint Laboratory of Environmental Simulation and Pollution Control, International Joint Laboratory for Regional Pollution Control, Ministry of Education, College of Environmental Sciences and Engineering, Peking University, Beijing, 100871, China

2 Department of Atmospheric and Oceanic Sciences, School of Physics, Peking University, Beijing, 100871, China

1 Measurement site.

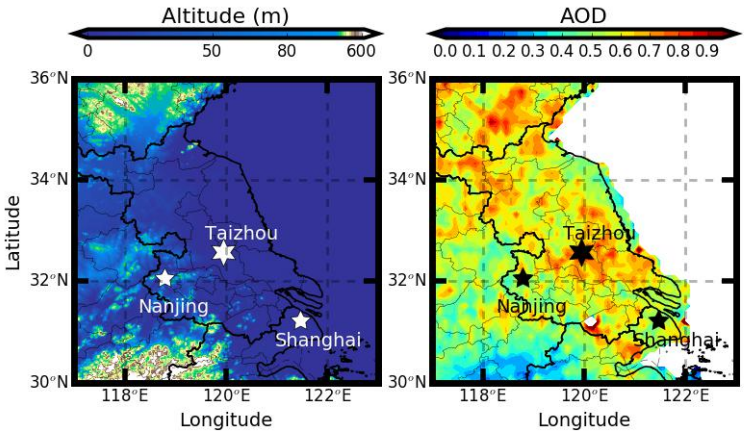

Figure S1: Measurement site of Taizhou (marked with stars). Filled colors represent (a) the topography of the Jianghuai Plain. (b) the average aerosol optical depth at 550nm during the year of 2017 from Moderate Resolution Imaging Spectroradiometer onboard satellite Aqua.

2 Instrument Setup

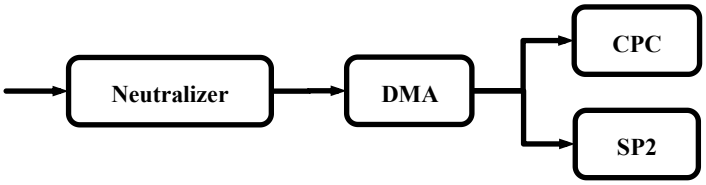

Figure S2. Schematic setup of the instrument.

A single particle soot photometer (SP2, Droplet Measurement Technologies, USA) was placed after a differential mobility analyzer (DMA, model 3081, TSI, USA) to measure the size-selected mixing states of the quasi monodisperse aerosols. The instrument setup was shown in Fig. S1. An SP2 in tandem with a DMA was used to measure the mixing states of monodisperse aerosols that pass through the DMA. A condensation particle counter (CPC, Model 3776, TSI, USA) was used to count aerosol number concentration with a flow ratio of 0.28 lpm in parallel with the SP2. The sheath flow of the DMA was 4 lpm. The DMA was set to scan the aerosols Dp from 12.3 to 697 nm over a period of 285 seconds and repeated after a pause of 15 seconds. More details of the instrument setup of the DMA-SP2-CPC system could refer to (Zhao et al., 2018). The mass concentrations of BC at a given Dp could be measured for every single particle.

3 Dataset from DMA-SP2-CPC system

When dealing with the measured signals from SP2, all aerosols were divided into two types: BC-contained aerosol and BC-free aerosol. Those aerosols were BC-contained when the measured amplitude of the incandescence signal strength by the wideband incandescence high gain channel of SP2 was higher than 50. The remaining particles were treated as BC-free aerosol because the amount of BC in the corresponding aerosol was zero or so small that was below the detection threshold of SP2.

3.1 Calibration of the SP2

Before measurement, calibrations were conducted to study the responses of the SP2 to the BC-contained aerosol and BC-free aerosol.

For the BC-contained aerosol, Aquadag soot particles with an effective density of 1.8 g/cm^3 were used. We manually changed Dps of the aerosol passing through the DMA from 80 to 400nm with a step of 20nm. Then the measured incandescence signal heights at different diameters were studied and the results were shown in Fig. S3. From fig. S3, the SP2 was not capable of measuring the Aquadag soot particles lower than 80 nm.

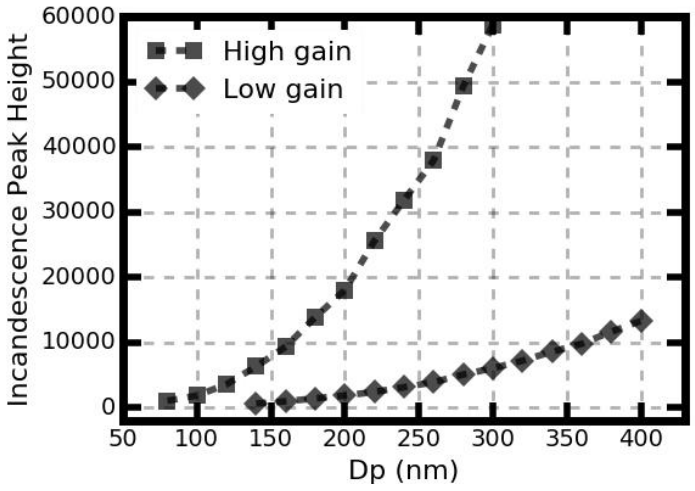

Figure S3. The calibrated relationship between the incandescence peak height and the BC diameter for both the incandescence high gain channel and the incandescence low gain

channel.

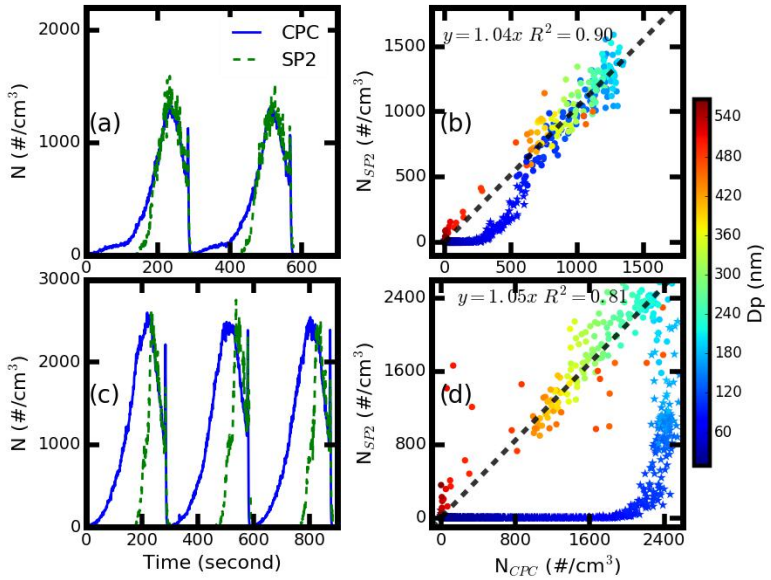

Figure. S4. (a) Measured time series by CPC and SP2 in blue solid line and green dashed line respectively for the Aquadag soot particles. (b) gives the comparison of the number concentration under different diameters. The diameter of these particles marked with circle and star is larger than 90 nm and lower than 90 nm respectively. (c) the same as (a), but for ammonia sulfate. (d) the same as (b), but for ammonia sulfate. The cut diameter for different markers is 180 nm. The slope in (b) and (d) are the results from these data marked with circles.

Another calibration study was carried out to determine the detecting efficiency of SP2. The DMA was set to scan from 10 nm to 567 nm over 5 minutes and the number concentrations measured CPC and SP2 were compared using ammonia sulfate and Aquadag soot particles separately. The calibration results were shown in Fig. S3. The measured number concentrations for SP2 and CPC showed good consistency when the particles were larger than 80 nm and 180 nm respectively for Aquadag soot particles and ammonia sulfate. In the following study, these particles with Dp larger than 80 nm and 180 nm for

BC-contained aerosols and BC-free particles respectively were considered.

3.2 Determine the effective density of the BC core

For the BC-containing aerosols, we assumed that these aerosols had a core-shell structure. The RI of the shell was assumed to be the same as that of the BC-free aerosols. Based on the field measurement results in the North China Plain from Zhang et al. (2016), the ambient BC core had an average density of about 1.2 g/cm3, indicating that ambient BC cores have a near-spherical shape with an internal void (air). The volume fraction of the void is defined as:

$$\mathrm{R}_{void} = 1 - \frac{D_e^3}{D_m^3} \qquad (7),$$

Where D_e is the non-void BC particle effective density calculated from the BC mass with the BC density of 1.8 g/cm3. D_m is BC particle mobility diameter. More definitions of the BC void can refer to the corresponding references (Zhang et al., 2016;Zhang et al., 2018).

The RI of the BC core ($m_2 = n_2 + k_2 i$) was calculated as the volume-weighted average between the RI of the void (air) (m_{air}) and rBC (m_{rBC}) by:

$$m_2 = m_{rBC} \times (1 - V_{air}) + m_{air} \times V_{air} \qquad (8),$$

where the value m_{rBC} was 2.26+1.26 i (Taylor et al., 2015); m_{air} was 1+0 i and V_{air} was the volume ratio of the internal voids in the rBC core. A density of 1.8 g/cm3 for the rBC core without the void (air) was used in this study (Bond and Bergstrom, 2006). For each of the given V_{air} and a given aerosol Dp, the Dc can be calculated. The corresponding thickness of the shell and the RIc can be determined. Then the σ_{abs} and σ_{sca} can be calculated using Mie scattering theory with the above Dc, shell thickness, and the RI for the core and the shell.

At the same time, the optical equivalent diameter can be derived from the measured light

scattering intensity using the leading-edge-only-fit method. Therefore, the corresponding void ratio can be constrained. Then the density of the core, the refractive index of the core can be calculated. More details of calculating the BC core effective density can refer to Zhang et al. (2018).

Based on the method above, we derived an effective density of 0.96 g/cm^3 of the BC core for the Taizhou site. The derived effective density of BC core for the Taizhou site is in accordance with that of Zhao et al. (2020).

3. 3 Multiple Charging Corrections

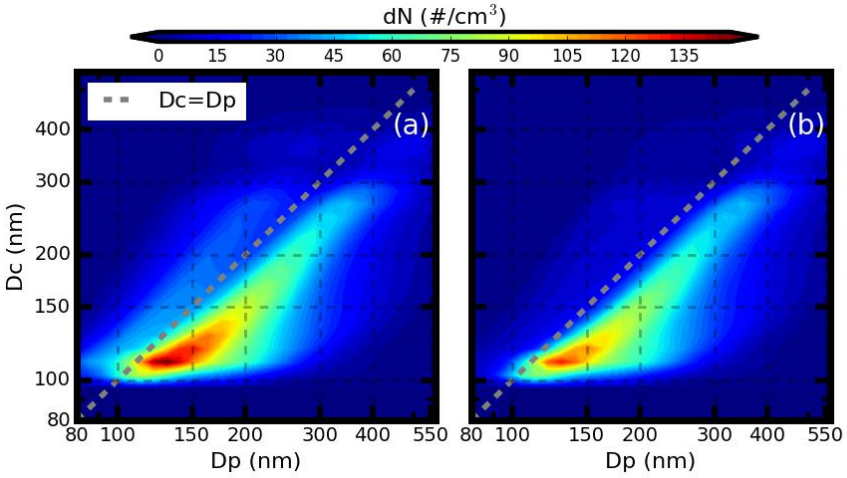

Figure S5. Measured number concentration distributions for different aerosol diameters with different core diameters for (a) multiple-charging uncorrected and (b) corrected.

Multiple charging corrections were conducted separately for BC-contained aerosol and BC-free particles. The distribution of BC-contained aerosol could be described using a two-variable with Dp and aerosol core diameter (Dc) described by $\frac{\partial N}{\partial \log(Dp)\partial \log(Dc)}$. The Dc was divided into 30 different bins from 80 to 500 nm, where the $\Delta \log Dc$ was the same for different bins. For each Dc bin, the number size distribution $\frac{\partial N}{\partial \log(Dp)}$ was distributed in one dimension in Dp. The multiple charging correction of one-dimensional size distribution had been well studied (Knutson and Whitby, 1975) and not detailed here. Therefore, the multiple

charging corrections for the two-dimensional distribution of BC-contained aerosol can be achieved. One example of the multiple charging corrections for the measured size distribution of BC-contained aerosols was shown in Fig. S4. Before corrections, there were a great number of particles that have Dc larger than Dp, which was mainly resulted from the multiple charging of aerosols that passing through the DMA. After the multiple charging corrections, both the amount and the shape of the distribution were changed. For the BC-free aerosols, the distribution was also one dimensional and the multiple charging corrections are easy to conduct.

4 Overview of the measurement

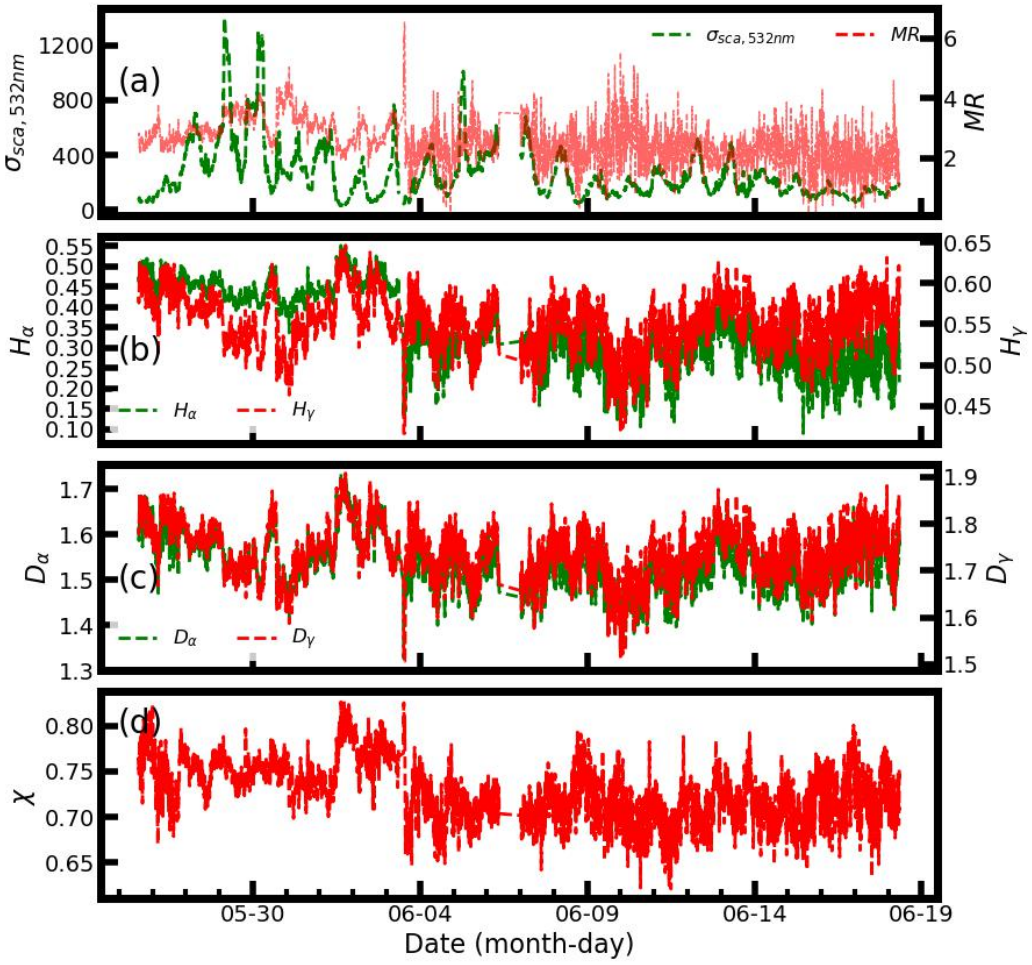

Figure S6. Measured time series of (a) σ_{sca} and MR, (b) H_α and H_γ, (c) D_α and D_γ, and (d) χ.

Bond, T. C., and Bergstrom, R. W.: Light Absorption by Carbonaceous Particles: An Investigative Review, Aerosol Sci. Technol., 40, 27-67, 10.1080/02786820500421521, 2006.

Knutson, E. O., and Whitby, K. T.: Aerosol classification by electric mobility: apparatus, theory, and applications, Journal of Aerosol Science, 6, 443-451, https://doi.org/10.1016/0021-8502(75)90060-9, 1975.

Taylor, J. W., Allan, J. D., Liu, D., Flynn, M., Weber, R., Zhang, X., Lefer, B. L., Grossberg, N., Flynn, J., and Coe, H.: Assessment of the sensitivity of core / shell parameters derived using the single-particle soot photometer to density and refractive index, Atmospheric Measurement Techniques, 8, 1701-1718, 10.5194/amt-8-1701-2015, 2015.

Zhang, Y., Zhang, Q., Cheng, Y., Su, H., Kecorius, S., Wang, Z., Wu, Z., Hu, M., Zhu, T., Wiedensohler, A., and He, K.: Measuring the morphology and density of internally mixed black carbon with SP2 and VTDMA: new insight into the absorption enhancement of black carbon in the atmosphere, Atmospheric Measurement Techniques, 9, 1833-1843, 10.5194/amt-9-1833-2016, 2016.

Zhang, Y., Su, H., Ma, N., Li, G., Kecorius, S., Wang, Z., Hu, M., Zhu, T., He, K., Wiedensohler, A., Zhang, Q., and Cheng, Y.: Sizing of ambient particles from a Single Particle Soot Photometer measurement to retrieve mixing state of Black Carbon at a Regional site of the North China Plain, Journal of Geophysical Research: Atmospheres, 123, 12778-12795, doi:10.1029/2018JD028810, 2018.

Zhao, G., Zhao, C., Zhao, W., and Hello, W.: Method to measure the size-resolved real part of aerosol refractive index, Atmos. Meas. Tech. Discuss., 2018, 1-20, 10.5194/amt-2018-399, 2018.

Zhao, G., Tan, T., Zhao, W., Guo, S., Tian, P., and Zhao, C.: A new parameterization scheme for the real part of the ambient urban aerosol refractive index, Atmos. Chem. Phys., 19, 12875-12885, 10.5194/acp-19-12875-2019, 2019.

Zhao, G., Li, F., and Zhao, C.: Determination of the refractive index of ambient aerosols, Atmospheric Environment, 240, 117800, https://doi.org/10.1016/j.atmosenv.2020.117800, 2020.